THE JOURNAL OF BIOLOGICAL CHEMISTRY VOL. 287, NO. 37, pp. 31270–31279, September 7, 2012

Regulation of the Subcellular Localization of the G-protein Subunit Regulator GPSM3 through Direct Association with 14-3-3 Protein*[S]

Received for publication, June 21, 2012, and in revised form, July 20, 2012 Published, JBC Papers in Press, July 26, 2012, DOI 10.1074/jbc.M112.394379

Patrick M. Giguère[‡], Geneviève Laroche[‡], Emily A. Oestreich[‡], Joseph A. Duncan[‡§], and David P. Siderovski[¶1]

From the [‡]Department of Pharmacology and [§]Division of Infectious Diseases, The University of North Carolina School of Medicine, Chapel Hill, North Carolina 27599-7365 and the [¶]Department of Physiology and Pharmacology, West Virginia University School of Medicine, Morgantown, West Virginia 26506

Background: GPSM3, a guanine nucleotide dissociation inhibitor acting on $G\alpha_i$ subunit family members, is both cytoplasm- and nucleus-localized.
Results: GPSM3 interacts directly with 14-3-3 through a phosphorylation-dependent mechanism.
Conclusion: Interaction with 14-3-3 stabilizes a cytoplasmic pool of GPSM3.
Significance: Our findings represent the first demonstration of post-translational modulation of GPSM3, a hematopoietic-restricted G-protein subunit regulator.

G-protein signaling modulator-3 (GPSM3), also known as G18 or AGS4, is a member of the $G\alpha_{i/o}$-Loco (GoLoco) motif containing proteins. GPSM3 acts through its two GoLoco motifs to exert GDP dissociation inhibitor activity over $G\alpha_i$ subunits; recently revealed is the existence of an additional regulatory site within GPSM3 directed toward monomeric $G\beta$ subunits during their biosynthesis. Here, using *in silico* and proteomic approaches, we have found that GPSM3 also interacts directly with numerous members of the 14-3-3 protein family. This interaction is dependent on GPSM3 phosphorylation, creating a mode II consensus 14-3-3 binding site. 14-3-3 binding to the N-terminal disordered region of GPSM3 confers stabilization from protein degradation. The complex of GPSM3 and 14-3-3 is exclusively cytoplasmic, and both moieties mutually control their exclusion from the nucleus. Phosphorylation of GPSM3 by a proline-directed serine/threonine kinase and the resultant association of 14-3-3 is the first description of post-translational regulation of GPSM3 subcellular localization, a process that likely regulates important spatio-temporal aspects of G-protein-coupled receptor signaling modulation by GPSM3.

G-protein-coupled receptors regulate numerous essential biological functions. They are key signal transducers of thousands of extracellular stimuli, regulating a plethora of cellular outcomes (1–4). Typically, during the cycle of activation, the ligand-occupied G-protein-coupled receptor promotes the exchange of guanosine diphosphate (GDP) for guanosine triphosphate (GTP) by the heterotrimeric G-protein α subunit. This active, GTP-bound $G\alpha$ subunit will thus dissociate from the $G\beta\gamma$ dimer and modulate intracellular effectors such as adenylyl cyclases and phospholipases (5, 6). Signal termination is regulated by the action of "regulator of G-protein signaling" (RGS) proteins that enhance the intrinsic GTPase activity of the $G\alpha$ subunit (7, 8). The inactive, GDP-bound $G\alpha$ subunit is generally thought to reassociate with the $G\beta\gamma$ dimer to form the inactive heterotrimer. However, a more recently discovered family of G-protein modulators, containing the conserved GoLoco[2] motif, also interacts with inactive, GDP-bound $G\alpha$ subunits of the G_i subfamily known to inhibit adenylyl cyclases (8–10). The GoLoco motif interaction inhibits spontaneous GDP release by the bound $G\alpha_i$ subunit (11, 12) and also occludes its $G\beta\gamma$ binding site (13), thereby inhibiting reassociation with $G\beta\gamma$ (14).

In mammalian cells, several different GoLoco motif-containing proteins are expressed, including RGS12 and -14, Rap1GAP, Pcp-2, AGS3, and LGN (8, 15–17). The latter protein is particularly important for spindle orientation during asymmetric cell division (reviewed in Ref. 10). Another protein containing this motif, called GPSM3, has a restricted expression profile to hematopoietic cell lineages (18–20). Recently, GPSM3 was found not only to modulate heterotrimeric G-protein subunit signaling through its two active GoLoco motifs, but also to affect monomeric $G\beta$ subunit biosynthesis and stability (20). In the same yeast two-hybrid screen that identified $G\beta$ subunits as GPSM3-interacting proteins (20), we also identified multiple isoforms of 14-3-3 as potential GPSM3 binding partners. 14-3-3 proteins are conserved regulatory molecules expressed in all eukaryotic cells (21, 22). Seven 14-3-3 isoforms

* This work was supported, in whole or in part, by National Institutes of Health Grants R01 GM082892 (to D. P. S.) and R01 AI088255 (to J. A. D.). This work was also supported by a Burroughs Wellcome Fund Career Award for Medical Scientists (to J. A. D.), NIAMS Postdoctoral Fellowship F32 AR057644 (to E. A. O.) from the National Institutes of Health, and postdoctoral fellowships from the Heart and Stroke Foundation of Canada and Fond de la recherche en santé Quebec (to P. M. G. and G. L.).
[S] This article contains supplemental Figs. S1–S3.
[1] To whom correspondence should be addressed: 3051 Health Sciences Center, One Medical Center Dr., Robert C. Byrd Health Sciences Center, Morgantown, WV 26506-9229. Tel.: 304-293-4991; E-mail: dpsiderovski@hsc.wvu.edu.

[2] The abbreviations used are: GoLoco, $G\alpha_{i/o}$-Loco; GPSM3, G-protein signaling modulator-3; GSK3, glycogen synthase kinase 3; BRET, bioluminescence resonance energy transfer; RLuc, *Renilla* luciferase; BiFC, bimolecular fluorescence complementation; Ni-NTA, nickel-nitrilotriacetic acid; pS, phosphoserine; SPR, surface plasmon resonance.

have been identified in mammals (α/β, γ, ϵ, δ/ζ, η, θ, and σ). 14-3-3 proteins are ubiquitously expressed, although different isoforms show some degree of tissue specificity (21). Multiple proteins have been reported to interact with 14-3-3 isoforms; these 14-3-3 interactors are known to regulate a wide range of cellular activities such as cell signaling, cytoskeleton organization, cellular trafficking, cell proliferation, apoptosis, metabolic pathways, and others (21, 22). Here, we have validated the GPSM3/14-3-3 interaction, mapped the region on GPSM3 critical for this interaction, and examined the relationship between both proteins on their subcellular localization.

EXPERIMENTAL PROCEDURES

Commercial Antibodies, Constructs, and Other Reagents—Horseradish peroxidase (HRP)-conjugated anti-hemagglutinin (HA) monoclonal antibody (clone 3F10) was obtained from Roche Applied Science. Anti-β-actin, anti-FLAG M2 antibody, and agarose-conjugated anti-FLAG M2 antibody were purchased from Sigma. HRP-conjugated goat anti-mouse and goat anti-rabbit antibodies were from GE Healthcare. Polyclonal pan anti-14-3-3 antibody was from Santa Cruz Biotechnology (Santa Cruz, CA). Monoclonal anti-GPSM3 antibody was produced in-house and has been previously described (20). All cDNAs used in this study were cloned in the pcDNA3.1 backbone vector (Invitrogen), with FLAG or HA epitope tag sequences included in the forward PCR primer to produce N-terminal tagged open reading frames as described previously (20) or in the reverse PCR primer to produce C-terminal tagged GSK3α. All mutagenesis was performed using the QuikChange site-directed mutagenesis kit following the manufacturer's recommendations (Agilent Technologies, Santa Clara, CA).

Cell Culture and Transfection—Human embryonic kidney 293 (HEK293) and THP-1 cell lines were each obtained from the American Type Culture Collection (ATCC) and maintained in DME medium or RPMI 1640 medium (Invitrogen), respectively, supplemented with 10% fetal bovine serum (Cellgro, Manassas, VA) at 37 °C in a humidified atmosphere containing 5% CO_2. Transient transfections of cell monolayers grown to 75–90% confluence were performed using Lipofectamine 2000 (Invitrogen) according to the manufacturer's instructions.

Immunoprecipitation and Immunoblotting—Cells were lysed with ice-cold lysis buffer (20 mM HEPES, pH 7.5, 1 mM EDTA, 150 mM NaCl, 1% Nonidet P-40, and Complete protease inhibitor mixture tablets (Roche Applied Science)) at 4 °C on a rocker platform for 30 min. Lysates were clarified by centrifugation at 16,000 $\times$ *g* for 15 min at 4 °C and quantified by the bicinchoninic acid (BCA) protein content assay (Pierce). For immunoprecipitation, lysates were incubated with specific antibody for 2 h at 4 °C followed by overnight incubation with protein-A/G agarose (Santa Cruz Biotechnology) or directly incubated with agarose-conjugated anti-FLAG M2 antibody overnight. Pelleted antibody/bead complexes were then washed three times with lysis buffer, and proteins were eluted in Laemmli buffer. Eluted proteins or lysate samples were resolved on 4–12% precast SDS-polyacrylamide gels (Novex/Invitrogen), transferred to nitrocellulose, immunoblotted using primary and HRP-conjugated secondary antibodies, and visualized by chemiluminescence (ECL, GE Healthcare).

Mass Spectrometry Analysis—Immunoprecipitation of FLAG-tagged GPSM3 and subsequent mass spectrometric identification of co-immunoprecipitating proteins were performed as described previously (20). For post-translational modification analysis, FLAG-tagged GPSM3 immunocomplex beads were submitted to the Systems Proteomics Center of University of North Carolina School (UNC)-Chapel Hill (directed by Dr. Oscar Alzate) and analyzed for post-translational modification using two-dimensional-differential in gel electrophoresis (23). Phosphorylation detected within GPSM3 was further analyzed using tandem mass spectrometry.

Bioluminescence Resonance Energy Transfer (BRET)—HEK293 cells were seeded in 12-well plates (3.5×10^5 cells/well) and transfected with a fixed amount of 14-3-3-RLuc vector DNA (50 ng), increasing amounts of GFP10-GPSM3 vector DNA (0–1500 ng), and corresponding (decreasing) amounts of pcDNA3 empty vector (1500–0 ng) to obtain a saturation curve. The other BRET assays were performed by transfecting cells with 50 ng of the *Renilla* luciferase (RLuc) fusion protein-expressing vector with 750 ng of GFP10 fusion protein expressing vector with 750 ng of additional "challenge" constructs or pcDNA3 vector. 24 h after transfection, cells were washed once, harvested, resuspended in BRET buffer (phosphate-buffered saline with 1 mM $CaCl_2$, 0.5 mM $MgCl_2$, 0.1% glucose), and distributed in white 96-well microplates. BRET was initiated by adding coelenterazine-400a at a final concentration of 5 μM. Measurements of emitted light were collected on a Mithras LB-940 plate reader (Berthold Technologies) using a $BRET^2$ filter set.

Bimolecular Fluorescence Complementation (BiFC)—Fusion constructs were made similar to those previously described for Gβ/GPSM3 tracking (20): namely, a fusion of the N-terminal fragment (amino acids 1–158) of yellow fluorescent protein (YN) to the N terminus of full-length GPSM3 (YN-GPSM3) and the C-terminal fragment (amino acids 159–238) of YFP (YC) to the C terminus of 14-3-3ζ (14-3-3-YC). HEK293 cells were transfected with an equal amount of plasmids encoding the fusion proteins YN-GPSM3 and 14-3-3-YC, and cells were incubated at 37 °C for 24 h. Total DNA quantity was normalized using empty pcDNA3.1 vector DNA. To measure fluorescence from formed complexes, transfected cells were washed, harvested, and resuspended in PBS. BiFC signal was acquired using a Mithras LB-940 plate reader using an excitation/emission filter set of 485 and 510 nm. The level of expression of each fusion protein was quantified by Western blotting using a polyclonal antibody directed against the GFP.

Immunofluorescence Microscopy—HEK293 cells were seeded in a 12-well plate and transfected with 0.4 μg of each DNA: YN-GPSM3 and 14-3-3-YC. The following day, cells were transferred to a poly-D-lysine-coated coverslip in a 6-well plate and grown overnight. Cells were then fixed with 4% paraformaldehyde plus PBS for 10 min at room temperature. Cells were then washed with PBS and permeabilized with 0.1% Triton X-100 plus PBS for 30 min at room temperature. Nonspecific binding was blocked with 0.1% Triton X-100 plus PBS containing 5% nonfat dry milk for 30 min at room temperature.

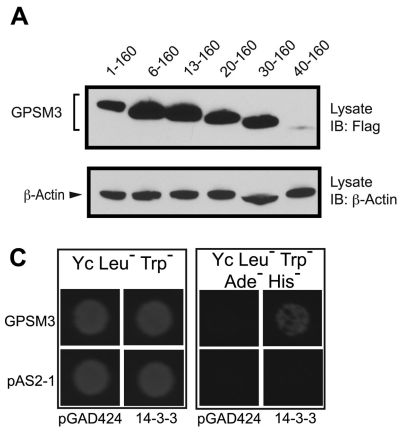

B

Identified proteins	Accession number	Number of clones
Gene_Symbol=YWHAB	IPI00216318	3
Gene_Symbol=YWHAH	IPI00216319	1
Gene_Symbol=YWHAE	IPI00000816	1
Gene_Symbol=YWHAZ	IPI00021263	2

D

Identified proteins	Accession number	Molecular Weight	Spectral Counts
Gene_Symbol=YWHAZ 14-3-3 protein zeta/delta	IPI00021263	28 kDa	16
Gene_Symbol=YWHAE 14-3-3 protein epsilon	IPI00000816	29 kDa	14
Gene_Symbol=YWHAQ 14-3-3 protein theta	IPI00018146	28 kDa	14
Gene_Symbol=YWHAB 14-3-3 protein beta/alpha	IPI00759832	28 kDa	13
Gene_Symbol=YWHAG 14-3-3 protein gamma	IPI00220642	28 kDa	11
Gene_Symbol=YWHAH 14-3-3 protein eta	IPI00216319	28 kDa	8

FIGURE 1. **Interaction between GPSM3 and multiple 14-3-3 family members.** *A*, truncation of the GPSM3 N terminus reveals a region between amino acids 31 and 40 essential for stable expression. HEK293 cells were transfected with N-terminal FLAG-tagged GPSM3 expression vectors encoding the indicated amino acid spans. Lysates were resolved by 4–12% SDS-PAGE and immunoblotted (*IB*) with anti-FLAG and anti-β-actin antibodies. *B*, a yeast two-hybrid screen was performed using full-length GPSM3 as bait on a human leukocyte cDNA library (20). Four different 14-3-3 isoforms, in single or multiple copies, were identified as shown. *C*, *Saccharomyces cerevisiae* yeast were co-transformed with the indicated bait plasmids (either expressing the Gal4p DNA binding domain alone (pAS2-1) or as a fusion with full-length GPSM3 (pAS2-1/GPSM3)) and prey plasmids (either expressing the Gal4p activation domain alone (pGAD424) or as a fusion with the entire human 14-3-3 α/β open reading frame (pACT2/14-3-3)). Transformed yeast were plated onto synthetic defined agar (*Yc*) lacking leucine (Leu^-, to select for the prey plasmid) and tryptophan (Trp^-, to select for the bait plasmid); growth on Yc Leu^- Trp^- medium demonstrates incorporation of both bait and prey plasmids (*left panel*). Growth on Yc Leu^- Trp^- medium also deficient in adenine (Ade^-) and histidine (His^-) indicates a positive protein-protein interaction (*right panel*). *D*, tandem mass spectrometry analysis confirmed the promiscuous interaction of GPSM3 with multiple isoforms of 14-3-3. Immunoprecipitated FLAG-GPSM3 and co-immunoprecipitated proteins were resolved by 4–12% SDS-PAGE, proteins visualized by SYPRO Ruby staining, and an apparent band at ~30–40 kDa was excised for LC/MS/MS peptide sequence identification. All 14-3-3 hits and their spectral counts are shown.

Cells were then incubated with an anti-HA FITC conjugate antibody (Roche Applied Science) for 1 h at room temperature in PBS supplemented with 5% nonfat dry milk. Cells were then washed three times with permeabilization buffer. Finally, coverslips were mounted using VECTASHIELD mounting medium containing DAPI (Vector Laboratories, Burlingame, CA) and examined by inverted fluorescence microscopy (Olympus IX70) using a 40× objective.

Protein Purification and Surface Plasmon Resonance—Full-length, N-terminal His-tagged, human 14-3-3ζ protein was produced recombinantly in bacteria from a pET vector-based prokaryotic expression construct using previously described cloning, expression, and purification techniques (24). His_6-GPSM3 protein from bacteria (pET-based vector) or Sf9 insect cells (pIEX-Bac3 based baculovirus) was purified by Ni-NTA affinity chromatography under denaturing conditions and refolded on-column with cold refolding buffer (20 mM HEPES, pH 7.5, 150 mM NaCl, 1% Nonidet P-40, 1 mM DTT). Protein was then eluted with refolding buffer containing 250 mM imidazole and buffer-exchanged into 20 mM HEPES, pH 7.5, 150 mM NaCl, 1 mM DTT, 30 mM CHAPS. Immobilization of His_6-14-3-3ζ and optical detection of protein binding via surface plasmon resonance (Biacore 3000; GE Healthcare) was conducted as described previously (24).

RESULTS AND DISCUSSION

Interaction between GPSM3 and 14-3-3 Family Members Stabilizes GPSM3—The N-terminal 50 amino acids of GPSM3 are of low complexity and predicted (44) to be disordered (*e.g.* supplemental Fig. S1). Truncation of the first 30 amino acids has little or no effect on ectopic GPSM3 expression (Fig. 1*A*). However, N-terminal deletion beyond 30 amino acids was observed to dramatically reduce levels of expressed GPSM3. Analysis of the primary sequence revealed the presence of a potential binding site for 14-3-3 between amino acids 31 and 40 (supplemental Fig. S2*A*). 14-3-3 binding sites are often localized within disordered regions of a protein; it is thought that interaction with disordered regions facilitates ligand capture and transition from a disordered to ordered state that stabilizes complex formation (25, 26).

As described previously (20), a yeast two-hybrid screen of a human leukocyte cDNA library was performed to identify novel interacting partners of GPSM3; as shown in Fig. 1*B*, numerous clones and isoforms of 14-3-3 were identified in this screen. Fig. 1*C* demonstrates the specific interaction between full-length GPSM3 used as bait and one of the retrieved 14-3-3 clones, identified as the full-length 14-3-3ζ isoform. An additional approach taken to identify GPSM3 binding partners, also described previously (20), employed tandem mass spectrometry identification of proteins present in an immunoprecipitated complex of ectopically expressed, FLAG-tagged GPSM3, confirming the presence of multiple isoforms of 14-3-3 (Fig. 1*D*).

14-3-3 proteins were initially discovered as phosphoserine-binding proteins, although phosphorylation-independent interactions have also been reported (22, 26). Consensus recognition motifs for 14-3-3 binding targets, although not absolute, are R(S/ϕ)(+)pSXP (mode I) and RX(ϕ/S)(+)(pS)XP (mode II) where pS is phosphoserine, + is a basic amino acid, ϕ is an aromatic residue, and X is any type of residue (25, 27). Analysis of the primary sequence of GPSM3 revealed three potential 14-3-3 interaction sites: site 1, R^{31}PWR^{34}SAP; site 2, RS^{54}AS^{56}LLS; and site 3, RS^{153}RPPT^{157}H (supplemental Fig. S2). The last two sites do not match perfectly with the consen-

sus motifs, but numerous 14-3-3 binding partners contain sequences that differ significantly from these optimal motifs (27). On the other hand, site 1 possesses all requirements for an optimal mode II 14-3-3 interaction (supplemental Fig. S1). Moreover, tandem mass spectrometry analyses of post-translational modifications on immunoprecipitated GPSM3 indicated that serines 35, 39, and 153 and threonine 157 are phosphorylated under basal conditions (*e.g.* supplemental Fig. S3). These two phosphorylated-residue clusters, Ser-35/Ser-39 and Ser-153/Thr-157, represent two of the three potential 14-3-3 interaction sites (namely, sites 1 and 3).

Mapping the Interaction between GPSM3 and 14-3-3 and Its Consequence on GPSM3 Stability—To confirm whether GPSM3 interacts with 14-3-3 proteins and identify the motif involved, we introduced point mutations into full-length, FLAG-tagged GPSM3 and its interaction with HA-tagged 14-3-3ζ was assessed by co-immunoprecipitation. We first observed that point mutation of arginines 31 and 34 (R31,34A),[3] serine 35 (S35A), or serine 39 (S39A) within GPSM3 each reduced the level of ectopically expressed GPSM3 protein observed (Fig. 2*A*); doubling the quantity of cDNA of each mutant resulted in a similar level of expression to that of wild-type GPSM3. We then used these altered transient transfection conditions to test their relative capability to co-immunoprecipitate with HA-tagged 14-3-3ζ. The R31,34A and S35A point mutants of GPSM3 failed to interact with 14-3-3ζ, and a considerable reduction of the interaction was observed with the S39A mutant (Fig. 2, *B* and *C*); these observations confirm site 1 of GPSM3 as important to the binding of 14-3-3. Mutations to GPSM3 residues R31,34 and Ser-35 were also seen to affect its interactions with the α/β and η isoforms of 14-3-3, whereas the S39A mutation reduced interaction with 14-3-3 α/β and ζ isoforms but had little effect with the 14-3-3 η isoform (Fig. 2, *C*, *D*, and *E*). As already described for other 14-3-3 substrates (27), mutation of GPSM3 residue serine 35 or 39 to aspartic acid was found to be ineffective in providing a phosphomimetic residue that enhances 14-3-3 binding (Fig. 2, *C*, *D*, and *E*). No effect on 14-3-3 binding was observed with S56A, S153A, or T157A mutations to GPSM3 (Fig. 2*B*), excluding the other two sites identified *in silico*.

Arginine 56 within 14-3-3ζ is essential for phosphoserine recognition (28–30). We observed that the interaction with wild-type GPSM3 was considerably reduced by introducing a R56A mutation into HA-tagged 14-3-3ζ (Fig. 2*F*); when combined with the partial loss-of-function S39A GPSM3 mutant, the R56A 14-3-3ζ mutation completely abolished the interaction (Fig. 2*F*).

Two additional point mutants of 14-3-3ζ isoforms have been well characterized; mutation of serine 58, known to be phosphorylated by PKA or PKB/AKT1, to alanine (S58A) induces constitutive dimerization of 14-3-3ζ, whereas mutation of this serine to aspartic acid (S58E) abrogates dimerization (31–33). However, as shown in Fig. 2*G*, neither of these mutations to serine 58 affected interaction with GPSM3, suggesting that the GPSM3 interaction with 14-3-3 is independent of the dimerization status of 14-3-3. Homo- and heterodimerization of 14-3-3 proteins is thought to be important for their cellular functions (33). The 14-3-3 dimer adopts a cup-like shape that can interact simultaneously with two binding sites within the same protein, thereby inducing conformational change and regulating protein activity or regulating other interactions via competition or occlusion. The presence of only one 14-3-3 binding site in GPSM3 and the binding of either dimeric or monomeric 14-3-3 to GPSM3 suggest that the 14-3-3 interaction could represent an important scaffolding function and/or stabilize formation of a multiprotein complex (21, 25).

The decreased stability of the 14-3-3 binding loss-of-function GPSM3 mutant R31,34A was further explored. FLAG-tagged GPSM3 was expressed in HEK293 cells in the presence or absence of 200 μg/ml cycloheximide to block *de novo* protein synthesis, and GPSM3 protein levels were subsequently tracked over time by Western blotting. Only prolonged incubation (>12 h) with cycloheximide was seen to dramatically reduce the protein level of wild-type GPSM3 (Fig. 3). In contrast, the R31,34A mutant of GPSM3 was found to have reduced expression following 6 h of cycloheximide treatment and was almost undetectable at 12 h after treatment (Fig. 3), indicating that the loss-of-function mutant has reduced stability as compared with wild-type GPSM3.

Endogenous GPSM3 Associates with Endogenous 14-3-3 in a Monocytic Cell Line—GPSM3 is proposed to be a hematopoietic restricted protein, and we have previously shown that the human monocytic cell line THP-1 expresses detectable levels of endogenous GPSM3 (20). The interaction between endogenous GPSM3 and 14-3-3 proteins was confirmed in THP-1 cells using co-immunoprecipitation with an in-house anti-GPSM3 monoclonal antibody as well as a polyclonal pan-14-3-3 antibody (Fig. 2*H*).

Characterization of the Interactions between GPSM3 and Its Binding Partners Using BRET—We also examined the interactions between GPSM3, 14-3-3, and G-protein subunits in a cellular context using BRET between RLuc- and green fluorescent protein (GFP10)-tagged fusions. Saturation BRET has been established as a robust measure of the specificity of an interaction (34). HEK293 cells transfected with a constant amount of 14-3-3-expressing donor construct (14-3-3-RLuc) and increasing amounts of the GPSM3 acceptor fusion expression vector (GFP10-GPSM3) were observed to produce a net BRET signal resulting in a saturable curve (Fig. 4*A*); mutation of the two arginines within the 14-3-3 binding site of GPSM3 (mutant R31,34A; Fig. 2*C*) eliminated BRET under the same experimental conditions (Fig. 4*A*). In addition, S35A and S39A point mutations within this site 1 in GPSM3 also greatly reduced the observed BRET signal as compared with the use of wild-type GPSM3 (Fig. 4*B*), confirming the results obtained by co-immunoprecipitation (Fig. 2*B*).

We previously reported that GPSM3 associates with heterotrimeric G-protein β subunits (Gβ) during their biosynthetic pathway toward formation of the Gβγ heterodimer (20). This GPSM3/Gβ interaction was found to be independent of the well established $G\alpha_i$/GDP interactions mediated by two of three GoLoco motifs within GPSM3 (19). We employed the BRET assay to evaluate the effect of 14-3-3 on both of these

[3] R31,34A = R31A and R34A.

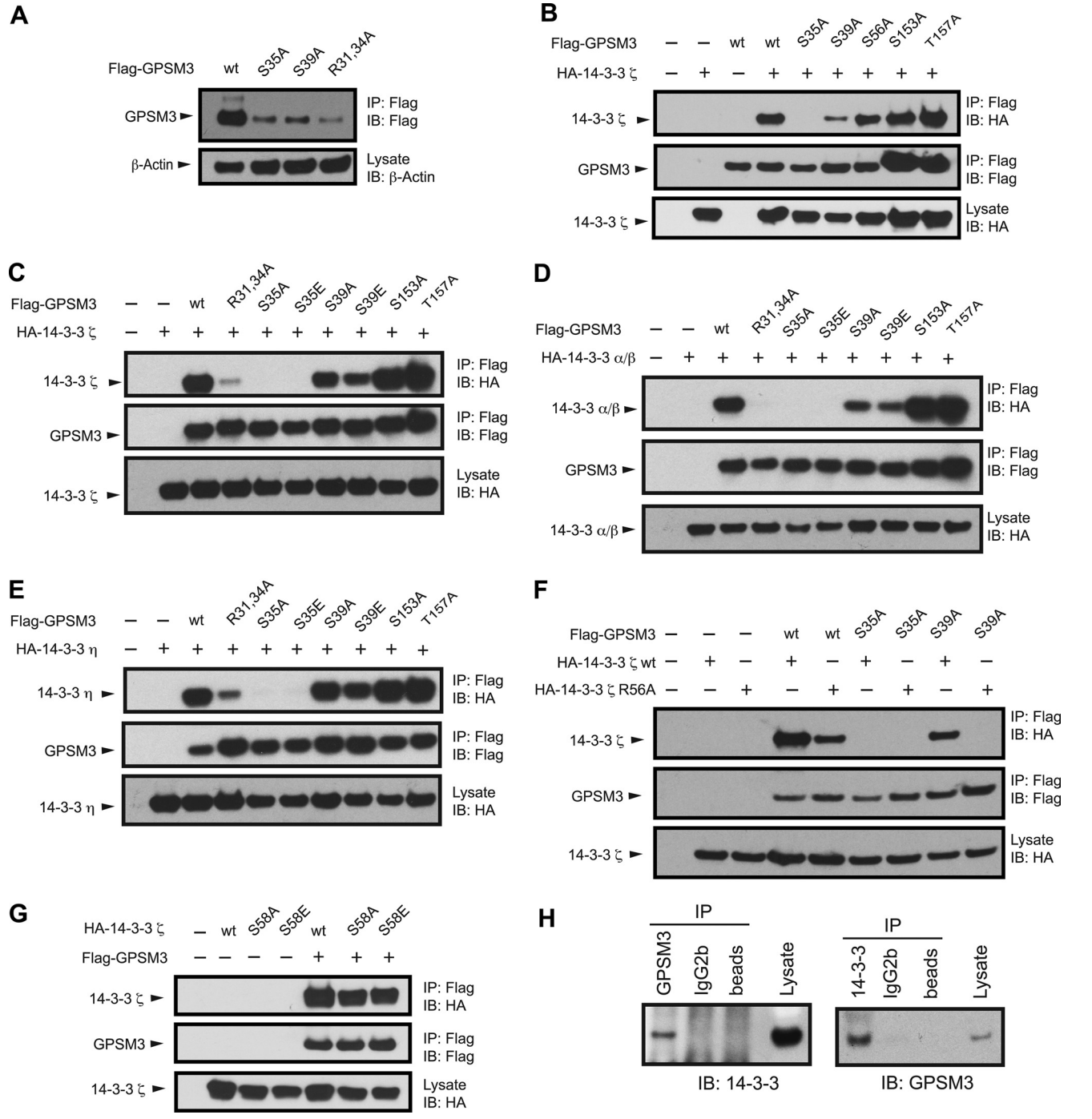

FIGURE 2. **Identification of the 14-3-3 binding motif within GPSM3 and the endogenous GPSM3/14-3-3 interaction within THP-1 cells.** *A*, point mutations within a region comprising amino acids 31 and 40 of GPSM3 perturb its stable expression. Mutagenized, FLAG-tagged GPSM3 expression constructs were transfected into HEK293 cells, and GPSM3 protein was immunoprecipitated (*IP*) using anti-FLAG M2 antibody. Immunoprecipitates were resolved by 4–12% SDS-PAGE and immunoblotted (*IB*) with anti-FLAG antibody. Lysates were resolved on 4–12% SDS-PAGE and immunoblotted with anti-β-actin as loading control. *B–E*, serines 35 and 39, as well as arginines 31 and 34, were identified as essential determinants for the interaction with 14-3-3 isoforms. Point-mutated, FLAG-tagged GPSM3 constructs were co-transfected with HA-tagged, wild type 14-3-3 ζ (*B* and *C*), α/β (*D*), η (*E*), 14-3-3ζ R56A mutant (*F*), and 14-3-3ζ S58A or S58E mutants (*G*); immunoprecipitation was performed as in *panel A* and immunoblotted with anti-HA- and anti-FLAG-HRP conjugates. *H*, detection of an endogenous GPSM3/14-3-3 interaction. Whole cell lysate from THP-1 cells was immunoprecipitated with the anti-GPSM3 mouse monoclonal antibody 35.5.1 (Ref. 20) or an IgG2 isotype control (*left panel*) or immunoprecipitated with the polyclonal pan anti-14-3-3 antibody or an IgG2 isotype control (*right panel*) and subsequently detected using the polyclonal pan anti-14-3-3 antibody (*left panel*) or anti-GPSM3 mouse monoclonal antibody 35.5.1 (*right panel*).

G-protein subunit interactions. Overexpression of 14-3-3 had no effect on the BRET ratio generated by co-expression of $G\alpha_{i1}$-RLuc/GFP10-GPSM3 fusion pairs or $G\beta_1$-RLuc/GFP10-GPSM3 fusion pairs (Fig. 4, *C* and *D*).

Conversely, overexpression of $G\beta_1$ was seen to greatly reduce the interaction between GPSM3 and 14-3-3, as shown both by BRET (Fig. 4*E*) and by co-immunoprecipitation studies (Fig. 4*F*). The mechanism underlying this unidirectional modulation

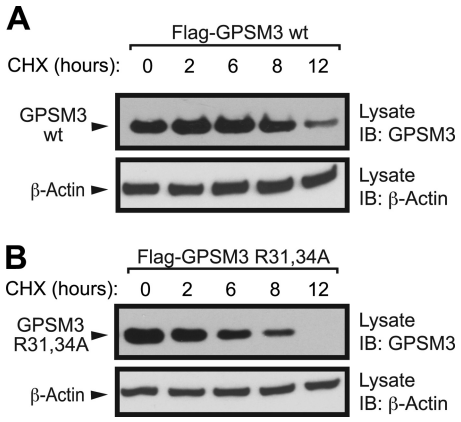

FIGURE 3. **Disruption of the interaction with 14-3-3 increases GPSM3 degradation.** HEK293 cells were transfected with FLAG-tagged GPSM3 wild type (*A*) or (R31,34A) (*B*) mutant. 24 h after transfection, cells were treated with cycloheximide (*CHX*, 200 μg/ml) for the indicated time prior to harvesting, and lysates were resolved on 4–12% SDS-PAGE and immunoblotted (*IB*) with anti-FLAG and anti-β-actin antibodies. *IP*, immunoprecipitated.

of the GPSM3/14-3-3 interaction by Gβ subunit expression, while 14-3-3 expression did not cause a reciprocal decrease in GPSM3/Gβ association, remains to be established, but it is unlikely to be direct steric competition between Gβ and 14-3-3 as this effect would have been seen to be bidirectional.

Direct Interaction between Recombinant GPSM3 and 14-3-3—To confirm the direct interaction between GPSM3 and 14-3-3, both proteins were first purified from recombinant expression systems. His-tagged 14-3-3ζ was expressed in *Escherichia coli*, purified by Ni-NTA affinity and size-exclusion chromatographies, and immobilized on a surface plasmon resonance (SPR) biosensor chip as described previously (24); the *E. coli*-derived 14-3-3ζ was dimeric, as assessed by migration during calibrated size-exclusion chromatography. Although GPSM3 was expressed and purified from *E. coli*, we also purified recombinant GPSM3 protein using baculovirus-mediated expression in Sf9 insect cells in which endogenous protein serine/threonine kinases are present. Recombinant GPSM3 purified from *E. coli* was observed to interact with immobilized 14-3-3ζ (Fig. 5*A*), but apparently with lower affinity than GPSM3 purified from insect cells; *i.e.* the Sf9-sourced protein bound immobilized 14-3-3ζ with higher apparent affinity (Fig. 5, *A* and *B*), suggesting its phosphorylation during insect cell expression. Given difficulties in attaining a true equilibrium state or single-phase association/dissociation kinetics using this SPR biosensor approach, we were unable to assign a numerical dissociation constant (K_D) value to the interaction using either equilibrium or kinetic approaches; however, based on the dose-response data obtained (*e.g.* Fig. 5*B*), we estimate the K_D for the GPSM3/14-3-3 interaction to be in the submicromolar range.

Analysis of the GPSM3/14-3-3 Interaction and Subcellular Localization by BiFC—BiFC is based on the reconstitution of two unfolded counterparts, such as the N- and C-terminal halves (YN and YC) of yellow fluorescent protein (YFP), to form a stable fluorescent protein. In addition to confirming the interaction between two proteins, the fluorescent signal generated can be used to locate the site of interaction within the cell by simple fluorescence microscopy visualization (35). For example, we previously used BiFC to show that the interaction between GPSM3 and Gβ subunits occurs in the cytoplasm and can also form juxtanuclear aggregates (20). Here, the N-terminal portion of YFP was fused to the N terminus of GPSM3 (YN-GPSM3), whereas the C-terminal fragment of YFP was fused to the C terminus of 14-3-3ζ (14-3-3-YC). Expression of each construct alone (YN-GPSM3 or 14-3-3-YC) or expression of each fusion paired with the cognate fluorescent protein fragment lacking the fusion bait gave no appreciable fluorescence, as expected. In contrast, combining expression of YN-GPSM3 with 14-3-3-YC generated a strong BiFC signal (Fig. 6*A*).

Co-expression of nontagged 14-3-3 significantly inhibited the BiFC signal (Fig. 6*A*), a measure of the specificity of the GPSM3/14-3-3 interaction. Unlike the interaction between GPSM3 and Gβ subunits that was found to lead to juxtanuclear aggregates over time (20), the interaction between GPSM3 and 14-3-3 observed by BiFC was diffusely located throughout the cytoplasm and completely excluded from the nucleus. This pattern of subcellular localization did not change over time after transfection and was not affected by the level of expression (*e.g.* Fig. 6*B*).

GPSM3 and 14-3-3 Mutually Affect Their Subcellular Localizations—GPSM3 expression has previously been observed throughout the cell including the nucleus, either when overexpressed or at the endogenous level (20); therefore, we next evaluated whether the interaction with 14-3-3 could regulate the subcellular localization of GPSM3. mCherry-tagged, wild-type GPSM3 was seen to be distributed throughout transfected cells, including the nucleus, but with a more pronounced cytoplasmic localization than that seen in the nucleus (Fig. 7*A*). In contrast, the 14-3-3 binding mutant of GPSM3 (R31,34A; as an mCherry fusion) was observed to be evenly distributed throughout transfected cells, without any distinction between nuclear and cytosolic compartments (Fig. 7*A*). The presence of ectopically expressed 14-3-3ζ increased the observed exclusion of wild-type GPSM3 from the nucleus (Fig. 7*B*, *panel ii*), but had no effect on the R31,34A mutant (Fig. 7*B*, *panel iii*). In these studies, we found HA-tagged 14-3-3ζ to be distributed throughout the cell when expressed alone (Fig. 7*B*, *panel i*) or with the loss-of-function R31,34A GPSM3 mutant (Fig. 7*B*, *panel iii*). On the other hand, HA-tagged 14-3-3ζ was excluded from the nucleus in the presence of wild type mCherry-GPSM3 (Fig. 7*B*, *panel ii*).

Involvement of GSK3α Kinase in the GPSM3/14-3-3 Interaction—Based on *in silico* prediction and mutagenesis as presented above, GPSM3 interacts with 14-3-3 through a mode II consensus 14-3-3 binding sequence $R^{31}PWR^{34}S^{35}AP$. Mutation of serine 35 completely abrogates the 14-3-3 interaction (*e.g.* Fig. 2, *B–F*), suggesting that phosphorylation of serine 35 is obligatory for 14-3-3 binding; the neighboring residue serine 39 also appears important as the interaction is greatly reduced when serine 39 is mutated (Fig. 2).

In silico analyses of potential serine/threonine kinases that could phosphorylate serine 35 (*e.g.* Scansite) reveal the mode II consensus 14-3-3 binding sequence within GPSM3 ($\underline{R^{31}PWR^{34}S^{35}AP}PS^{39}PP$) as overlapping with a consensus site for the glycogen synthase kinase 3 (GSK3) substrates ((S/T)*XXX*($\underline{pS/T}$); Ref. 36), where the first S/T is the GSK3 phos-

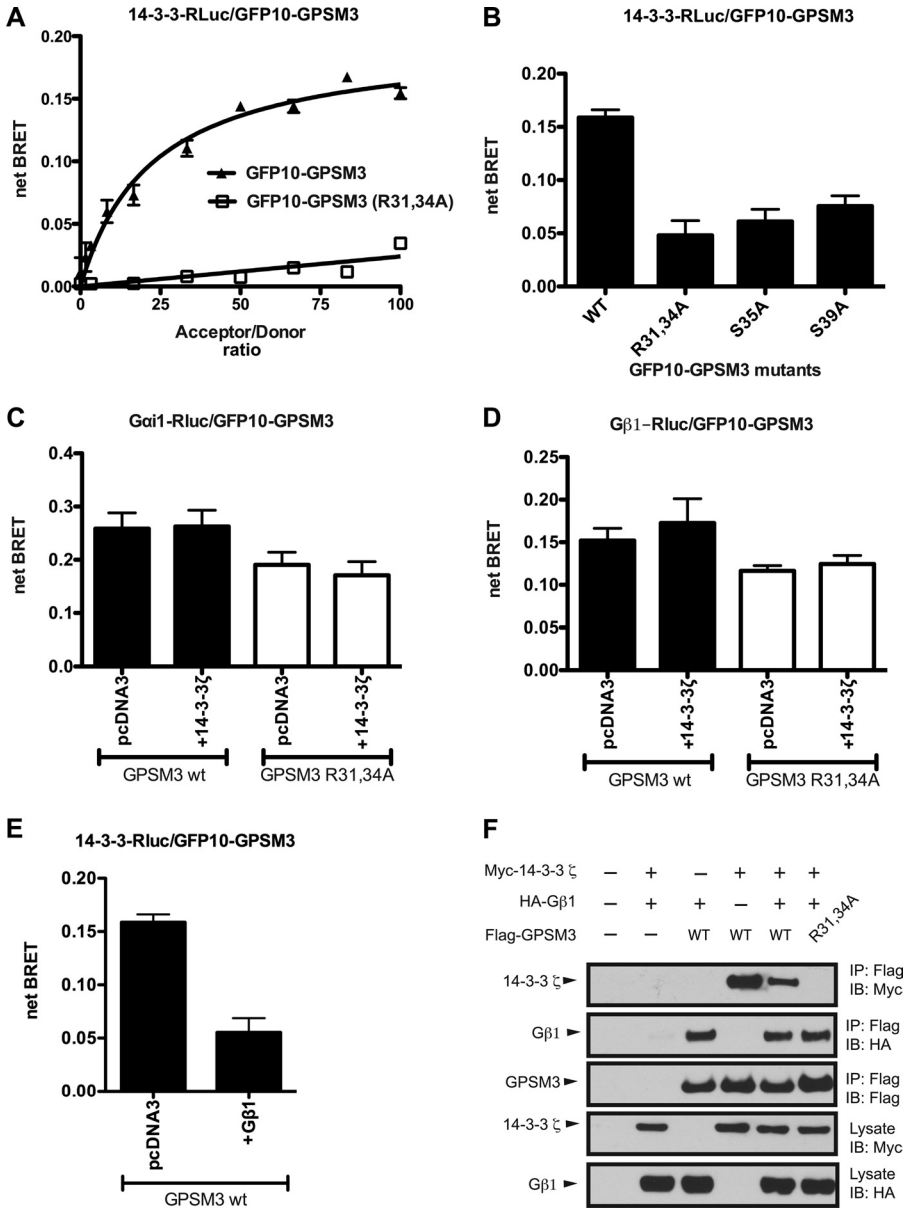

FIGURE 4. **Characterization of the GPSM3/14-3-3 interaction using BRET.** *A*, the interaction between GPSM3 and 14-3-3 was confirmed by a BRET saturation experiment. A constant amount of 14-3-3-RLuc fusion expression vector was co-transfected into HEK293 cells with increasing amounts of GFP10-GPSM3 fusion expression vector; the resultant net BRET ratio was plotted as a function of the acceptor/donor ratio. The specificity of the interaction is indicated by the saturable nature of the BRET signal. *B*, point mutations, previously found by co-immunoprecipitation to disrupt ((S35A) or (R31,34A)) or strongly reduce (S39A) the GPSM3 interaction with 14-3-3, were introduced in the GFP10-GPSM3 construct and assayed by BRET for 14-3-3 interaction. *C* and *D*, the effect of 14-3-3 on the previously described interactions between GPSM3 and $G\alpha_{i1}$ or $G\beta_1$ (20) was assayed by BRET. $G\alpha_{i1}$-RLuc or $G\beta_1$-Rluc expression constructs were co-transfected in HEK293 cells with GFP10-GPSM3 (wild type or R31,34A mutant) in the presence or absence of 14-3-3ζ expression vector. *E* and *F*, $G\beta_1$ overexpression reduces interaction between GPSM3 and 14-3-3. *E*, nontagged $G\beta_1$ was co-expressed with the 14-3-3-RLuc/GFP10-GPSM3 BRET pair, and the effect on BRET signal was measured. *Error bars* in *panels A–E* indicate S.E. *F*, FLAG-tagged GPSM3 (WT or R31,34A) constructs were co-transfected with HA-tagged, wild-type 14-3-3ζ expression vector in the presence or absence of HA-tagged $G\beta_1$, and immunoprecipitation was performed using agarose-conjugated anti-FLAG M2 antibody. Immunoprecipitates (*IP*) were resolved on a 4–12% SDS-PAGE and immunoblotted (*IB*) with anti-HA- and anti-FLAG-HRP conjugates.

phorylation target, *X* is any amino acid, and pS/T is the priming phosphorylation site. GSK3 has an unusual preference for substrates that are prephosphorylated at a priming, C-terminal Ser/Thr residue; this priming process, although not strictly required, increases phosphorylation efficiency of the N-terminal Ser/Thr by 100–1000-fold (37). Moreover, GSK3 favors the presence of proline in the recognition site; for example, one of the GSK3 phosphorylation sites in glycogen synthase is SVPPpS (38). GPSM3 serine 35, required for the 14-3-3 interaction, fits perfectly into this GSK3 recognition sequence. Furthermore, serine 39 was found to be phosphorylated in the mass spectrometry analysis of GPSM3 post-translational modifications (supplemental Fig. S3), and mutation of the serine 39 to alanine (S39A) reduces the GPSM3/14-3-3 interaction. As GPSM3 serine 39 is followed by a proline, we focused our studies on GSK3, a potential proline-directed kinase (39–41), and other well characterized, proline-directed serine/threonine kinases (*e.g.* cyclin-dependent kinases (CDKs), c-Jun N-terminal kinases (JNKs), p38, and extracellular-signal-regulated kinases 1/2 (ERK1/2).

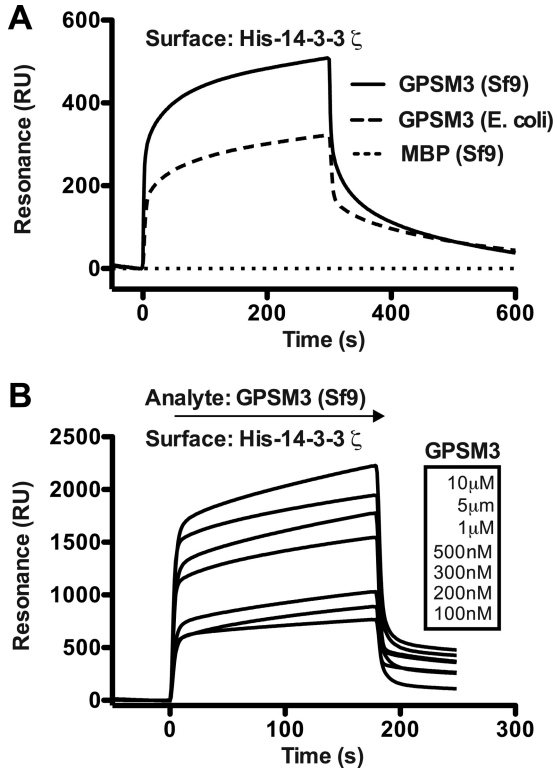

FIGURE 5. **Confirmation of the direct interaction between GPSM3 and 14-3-3 by SPR.** *A*, recombinant 14-3-3ζ purified from *E. coli* was covalently immobilized on a nickel-NTA SPR chip and recombinant GPSM3, purified either from a bacterial (*E. coli*) or from an insect cell (Sf9) source, was superfused over the biosensor surface at 250 nM for 300 s. *RU*, resonance units; *MBP*, maltose binding protein. *B*, SPR interaction experiment was performed as in *panel A*, but with the indicated concentrations of Sf9-sourced recombinant GPSM3 protein and a 180-s association time.

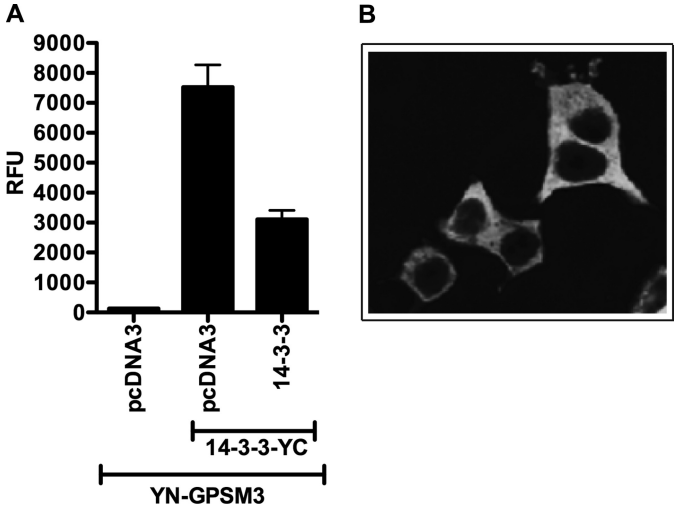

FIGURE 6. **Analysis of the GPSM3 and 14-3-3 interaction using BiFC.** *A* and *B*, HEK293 were transfected with plasmids expressing YN-GPSM3 (amino acids 1–158 of YFP fused to GPSM3) and 14-3-3-YC (14-3-3ζ fused to amino acids 159–238 of YFP), and the fluorescence from the assembled YFP fluorophore was assayed at 24 h after transfection. *A*, cells were harvested, and fluorescence was quantified on a plate reader. Total DNA used for transfection was normalized using empty pcDNA3.1 vector DNA. *Error bars* indicate S.E. *RFU*, relative fluorescence units. *B*, epifluorescence microscopy images of HEK293 cells transfected with plasmids expressing the two YFP protein fragment fusions as in *panel A* show an exclusively cytoplasmic localization of the reconstituted fluorescent complex.

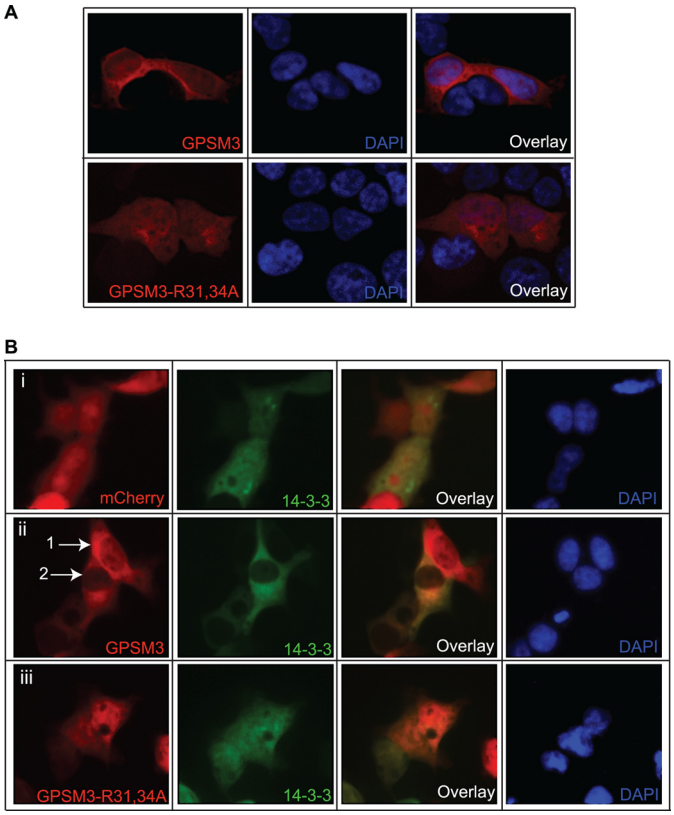

FIGURE 7. **GPSM3 and 14-3-3 mutually regulate their subcellular localization.** HEK293 were transfected with mCherry-tagged GPSM3 (either wild type or R31,34A mutant) or nontagged mCherry expression vectors in the absence (*A*) or presence (*B*) of HA-tagged 14-3-3ζ (*green*) expression vector. After 24 h, cells were fixed and labeled with an anti-HA-FITC antibody conjugate and mounted with VECTASHIELD containing the nuclear stain DAPI (*blue*). *A*, mCherry-GPSM3 (wild type) was found to have a prominent cytosolic localization as compared with the (R31,34A) variant. *B*, co-expression of 14-3-3ζ increased the cytosolic partitioning of mCherry-GPSM3 (wild type), but not of the (R31,34A) mutant. Similarly, co-expression of mCherry-GPSM3 (wild type) induced nuclear exclusion of the subcellular localization of 14-3-3ζ as compared with co-expression of the (R31,34A) mutant or nontagged mCherry protein. Cell numbering in *panel B* (*panel ii*) indicates (**1**) a cell expressing solely mCherry-GPSM3 *versus* (**2**) a cell in the same field co-expressing mCherry-GPSM3 and HA-14-3-3ζ. Note the heightened degree of nuclear exclusion of wild-type mCherry-GPSM3 expression in cell **2** *versus* cell **1**. Cells imaged are representative of the majority of cells present.

As shown in Fig. 8*A*, neither U0126 (MEK1/2 inhibitor, an upstream activator of ERK1/2) nor SB203580 (p38α/β inhibitor) had any effect on GPSM3 expression levels, even at high concentration (10 μM). SP600125 (JNK inhibitor), olomoucine (CDK inhibitor), and H89 (a broad range inhibitor often used to inhibit PKA) were each seen to reduce GPSM3 expression levels. Most dramatically, the GSK3α/β inhibitor (SB216763) was found to profoundly reduce the level of ectopic GPSM3 expression (Fig. 8*A*).

A similar effect was observed on endogenous GPSM3 expression in THP-1 cells, with expression reduced by more than 75% (Fig. 8*B*). None of the other, above mentioned inhibitors were seen to have any effect on endogenous GPSM3 levels in THP-1 cells, although H89 treatment was found to drastically reduce THP-1 cell viability.

Mammalian cells express two isoforms of GSK3, GSK3α and GSK3β, which share 98% sequence similarity in their kinase domain. However, the isoforms are structurally and functionally distinct (42). There is an N-terminal glycine-rich extension in

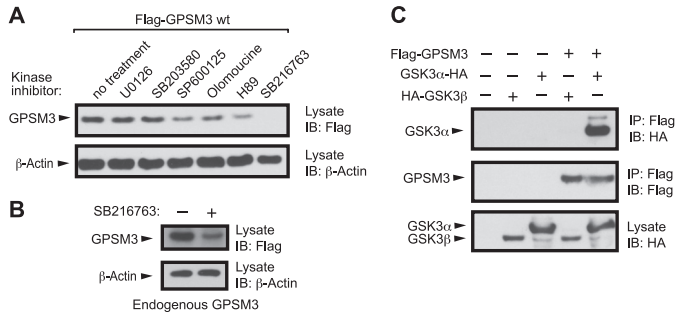

FIGURE 8. **Inhibition of GSK3 reduces GPSM3 protein expression and GSK3α forms a complex with GPSM3.** *A*, HEK293 cells transfected with FLAG-tagged, wild-type GPSM3 were incubated 12–16 h with the indicated kinase inhibitors at 10 μM. Lysates were resolved on 4–12% SDS-PAGE and immunoblotted (*IB*) with anti-FLAG and anti-β-actin antibodies. *B*, THP-1 cells were incubated 16 h with the GSK3 kinase inhibitor SB216763 at 10 μM, and lysates were analyzed by immunoblot with anti-GPSM3 mouse monoclonal antibody and anti-β-actin. *C*, HEK293 cells were co-transfected with FLAG-tagged GPSM3 and HA-GSK3β or GSK3α-HA expression constructs, and immunoprecipitation (*IP*) was performed using agarose-conjugated anti-FLAG M2 antibody. Immunoprecipitates were resolved by 4–12% SDS-PAGE and immunoblotted with anti-HA- and anti-FLAG-HRP conjugates.

GSK3α as well as distinct C-terminal regions (only 38% similarity between isoforms). When co-expressed in HEK293 cells, GSK3α, but not GSK3β, was found in complex with FLAG-tagged GPSM3 (Fig. 8*C*). The exclusion of GSK3β, even when overexpressed, highlights the unique nature and specificity of this GSK3α/GPSM3 interaction. To date, only the protein adaptor RACK1 has been shown to selectively interact with GSK3α, an interaction that involves the unique N-terminal extension of GSK3α (43). The mechanism by which GSK3α is recruited to GPSM3 as well as the regulation of this interaction is unknown.

Conclusions—A single 14-3-3 binding site exists in GPSM3 and corresponds to a consensus mode II binding motif, R*X*(ϕ/S)(+)(pS)*X*P, in which position P_0 is an obligatory pS known to interact with positively charged arginine 56 and 127 within the 14-3-3 binding groove (ζ isoform numbering). The arginine at position P_{-4} forms an intramolecular salt bridge with the P_0 phosphoserine, and the proline at position P_{+2} orients the main chain direction of the binding peptide (25). The binding site within GPSM3 (RPWRS^{35}AP) contains all requirements for an optimal, high affinity interaction; mutagenesis confirmed the critical role of these elements as the R31,34A and S35A mutants of GPSM3 completely abolish interaction with 14-3-3. Additionally, the R56A 14-3-3 mutant exhibited reduced interaction with GPSM3. Co-immunoprecipitation of endogenous GPSM3 and 14-3-3 proteins from the human monocytic cell line THP-1 suggests basal phosphorylation of GPSM3 at serine 35 as potentially mediated by GSK3α. The GPSM3/14-3-3 interaction is seen to stabilize GPSM3 from degradation and also support the nuclear exclusion of both proteins. Future studies will be directed at establishing the specific roles of these newly described 14-3-3 and GSK3α interactions in the G-protein modulatory functions of GPSM3 within immune system cells.

Acknowledgments—We thank Dr. N. A. Lambert (Georgia Health Sciences University) for advice regarding BRET studies. The GFP10-Gβ_1 construct and BiFC backbone vectors were kind gifts of Dr. Denis J. Dupré (Dalhousie University).

REFERENCES

1. Bockaert, J., and Pin, J. P. (1999) Molecular tinkering of G protein-coupled receptors: an evolutionary success. *EMBO J.* **18,** 1723–1729
2. Gurevich, V. V., and Gurevich, E. V. (2008) Rich tapestry of G protein-coupled receptor signaling and regulatory mechanisms. *Mol. Pharmacol.* **74,** 312–316
3. Luttrell, L. M. (2008) Reviews in molecular biology and biotechnology: transmembrane signaling by G protein-coupled receptors. *Mol. Biotechnol.* **39,** 239–264
4. McCoy, K. L., and Hepler, J. R. (2009) Regulators of G protein signaling proteins as central components of G protein-coupled receptor signaling complexes. *Prog. Mol. Biol. Transl. Sci.* **86,** 49–74
5. Chung, K. Y., Rasmussen, S. G., Liu, T., Li, S., DeVree, B. T., Chae, P. S., Calinski, D., Kobilka, B. K., Woods, V. L., Jr., and Sunahara, R. K. (2011) Conformational changes in the G protein G_s induced by the β2 adrenergic receptor. *Nature* **477,** 611–615
6. Offermanns, S. (2003) G-proteins as transducers in transmembrane signaling. *Prog. Biophys. Mol. Biol.* **83,** 101–130
7. Neubig, R. R., and Siderovski, D. P. (2002) Regulators of G-protein signaling as new central nervous system drug targets. *Nat. Rev. Drug Discov.* **1,** 187–197
8. Siderovski, D. P., and Willard, F. S. (2005) The GAPs, GEFs, and GDIs of heterotrimeric G-protein α subunits. *Int. J. Biol. Sci.* **1,** 51–66
9. Sato, M., Blumer, J. B., Simon, V., and Lanier, S. M. (2006) Accessory proteins for G-proteins: partners in signaling. *Annu. Rev. Pharmacol. Toxicol.* **46,** 151–187
10. Willard, F. S., Kimple, R. J., and Siderovski, D. P. (2004) Return of the GDI: the GoLoco motif in cell division. *Annu. Rev. Biochem.* **73,** 925–951
11. Kimple, R. J., De Vries, L., Tronchère, H., Behe, C. I., Morris, R. A., Gist Farquhar, M., and Siderovski, D. P. (2001) RGS12 and RGS14 GoLoco motifs are $G\alpha_i$ interaction sites with guanine nucleotide dissociation inhibitor activity. *J. Biol. Chem.* **276,** 29275–29281
12. Peterson, Y. K., Bernard, M. L., Ma, H., Hazard, S., 3rd, Graber, S. G., and Lanier, S. M. (2000) Stabilization of the GDP-bound conformation of $G_i\alpha$ by a peptide derived from the G-protein regulatory motif of AGS3. *J. Biol. Chem.* **275,** 33193–33196
13. Kimple, R. J., Kimple, M. E., Betts, L., Sondek, J., and Siderovski, D. P. (2002) Structural determinants for GoLoco-induced inhibition of nucleotide release by Gα subunits. *Nature* **416,** 878–881
14. Webb, C. K., McCudden, C. R., Willard, F. S., Kimple, R. J., Siderovski, D. P., and Oxford, G. S. (2005) D_2 dopamine receptor activation of potassium channels is selectively decoupled by Gα-specific GoLoco motif peptides. *J. Neurochem.* **92,** 1408–1418
15. Ponting, C. P. (1999) Raf-like Ras/Rap binding domains in RGS12- and still-life-like signaling proteins. *J. Mol. Med.* **77,** 695–698
16. Siderovski, D. P., Diversé-Pierluissi, M., and De Vries, L. (1999) The GoLoco motif: a $G\alpha_{i/o}$ binding motif and potential guanine-nucleotide exchange factor. *Trends Biochem. Sci.* **24,** 340–341
17. Takesono, A., Cismowski, M. J., Ribas, C., Bernard, M., Chung, P., Hazard, S., 3rd, Duzic, E., and Lanier, S. M. (1999) Receptor-independent activators of heterotrimeric G-protein signaling pathways. *J. Biol. Chem.* **274,** 33202–33205
18. Cao, X., Cismowski, M. J., Sato, M., Blumer, J. B., and Lanier, S. M. (2004) Identification and characterization of AGS4: a protein containing three G-protein regulatory motifs that regulate the activation state of $G_i\alpha$. *J. Biol. Chem.* **279,** 27567–27574
19. Kimple, R. J., Willard, F. S., Hains, M. D., Jones, M. B., Nweke, G. K., and Siderovski, D. P. (2004) Guanine nucleotide dissociation inhibitor activity of the triple GoLoco motif protein G18: alanine-to-aspartate mutation restores function to an inactive second GoLoco motif. *Biochem. J.* **378,** 801–808
20. Giguère, P. M., Laroche, G., Oestreich, E. A., and Siderovski, D. P. (2012) G-protein signaling modulator-3 regulates heterotrimeric G-protein dynamics through dual association with Gβ and $G\alpha_i$ protein subunits. *J. Biol. Chem.* **287,** 4863–4874
21. Sun, S., Wong, E. W., Li, M. W., Lee, W. M., and Cheng, C. Y. (2009) 14-3-3 and its binding partners are regulators of protein-protein interactions

during spermatogenesis. *J. Endocrinol.* **202,** 327–336
22. Freeman, A. K., and Morrison, D. K. (2011) 14-3-3 proteins: diverse functions in cell proliferation and cancer progression. *Semin. Cell Dev. Biol.* **22,** 681–687
23. Diez, R., Herbstreith, M., Osorio, C., and Alzate, O. (2010) 2-D fluorescence difference gel electrophoresis (DIGE) in neuroproteomics. in *Neuroproteomics* (Alzate, O. ed), pp. 51–70, CRC Press, Boca Raton, FL
24. Kimple, A. J., Muller, R. E., Siderovski, D. P., and Willard, F. S. (2010) A capture coupling method for the covalent immobilization of hexahistidine-tagged proteins for surface plasmon resonance. *Methods Mol. Biol.* **627,** 91–100
25. Obsil, T., and Obsilova, V. (2011) Structural basis of 14-3-3 protein functions. *Semin. Cell Dev. Biol.* **22,** 663–672
26. Bustos, D. M. (2012) The role of protein disorder in the 14-3-3 interaction network. *Mol. Biosyst.* **8,** 178–184
27. Johnson, C., Crowther, S., Stafford, M. J., Campbell, D. G., Toth, R., and MacKintosh, C. (2010) Bioinformatic and experimental survey of 14-3-3 binding sites. *Biochem. J.* **427,** 69–78
28. Rittinger, K., Budman, J., Xu, J., Volinia, S., Cantley, L. C., Smerdon, S. J., Gamblin, S. J., and Yaffe, M. B. (1999) Structural analysis of 14-3-3 phosphopeptide complexes identifies a dual role for the nuclear export signal of 14-3-3 in ligand binding. *Mol. Cell* **4,** 153–166
29. Petosa, C., Masters, S. C., Bankston, L. A., Pohl, J., Wang, B., Fu, H., and Liddington, R. C. (1998) 14-3-3ζ binds a phosphorylated Raf peptide and an unphosphorylated peptide via its conserved amphipathic groove. *J. Biol. Chem.* **273,** 16305–16310
30. Yaffe, M. B., Rittinger, K., Volinia, S., Caron, P. R., Aitken, A., Leffers, H., Gamblin, S. J., Smerdon, S. J., and Cantley, L. C. (1997) The structural basis for 14-3-3:phosphopeptide binding specificity. *Cell* **91,** 961–971
31. Powell, D. W., Rane, M. J., Chen, Q., Singh, S., and McLeish, K. R. (2002) Identification of 14-3-3ζ as a protein kinase B/Akt substrate. *J. Biol. Chem.* **277,** 21639–21642
32. Woodcock, J. M., Murphy, J., Stomski, F. C., Berndt, M. C., and Lopez, A. F. (2003) The dimeric versus monomeric status of 14-3-3ζ is controlled by phosphorylation of Ser-58 at the dimer interface. *J. Biol. Chem.* **278,** 36323–36327
33. Gu, Y. M., Jin, Y. H., Choi, J. K., Baek, K. H., Yeo, C. Y., and Lee, K. Y. (2006) Protein kinase A phosphorylates and regulates dimerization of 14-3-3ϵ. *FEBS Lett.* **580,** 305–310
34. Mercier, J. F., Salahpour, A., Angers, S., Breit, A., and Bouvier, M. (2002) Quantitative assessment of β1- and β2-adrenergic receptor homo- and heterodimerization by bioluminescence resonance energy transfer. *J. Biol. Chem.* **277,** 44925–44931
35. Kerppola, T. K. (2008) Bimolecular fluorescence complementation (BiFC) analysis as a probe of protein interactions in living cells. *Annu. Rev. Biophys.* **37,** 465–487
36. Sutherland, C. (2011) What Are the *bona fide* GSK3 Substrates? *Int. J. Alzheimers Dis.* **2011,** 505607
37. Thomas, G. M., Frame, S., Goedert, M., Nathke, I., Polakis, P., and Cohen, P. (1999) A GSK3-binding peptide from FRAT1 selectively inhibits the GSK3-catalyzed phosphorylation of axin and β-catenin. *FEBS Lett.* **458,** 247–251
38. Dajani, R., Fraser, E., Roe, S. M., Young, N., Good, V., Dale, T. C., and Pearl, L. H. (2001) Crystal structure of glycogen synthase kinase 3β: structural basis for phosphate-primed substrate specificity and autoinhibition. *Cell* **105,** 721–732
39. Jope, R. S., and Johnson, G. V. (2004) The glamour and gloom of glycogen synthase kinase-3. *Trends Biochem. Sci.* **29,** 95–102
40. Ubersax, J. A., and Ferrell, J. E., Jr. (2007) Mechanisms of specificity in protein phosphorylation. *Nat. Rev. Mol. Cell Biol.* **8,** 530–541
41. Cohen, P., and Frame, S. (2001) The renaissance of GSK3. *Nat. Rev. Mol. Cell Biol.* **2,** 769–776
42. Doble, B. W., and Woodgett, J. R. (2003) GSK-3: tricks of the trade for a multitasking kinase. *J. Cell Sci.* **116,** 1175–1186
43. Zeidner, L. C., Buescher, J. L., and Phiel, C. J. (2011) A novel interaction between glycogen synthase kinase-3α (GSK-3α) and the scaffold protein receptor for activated C-kinase 1 (RACK1) regulates the circadian clock. *Int. J. Biochem. Mol. Biol.* **2,** 318–327
44. Linding, R., Russell, R. B., Neduva, V., and Gibson, T. J. (2003) GlobPlot: exploring protein sequences for globularity and disorder. *Nucleic Acids Res.* **31,** 3701–3708